THE BALTIC JOURNAL
OF ROAD AND BRIDGE ENGINEERING

ISSN 1822-427X / eISSN 1822-4288
2017 Volume 12(1): 38–47

STEREO VISION METHOD APPLICATION TO ROAD INSPECTION

Marcin Staniek

Dept of Transport Systems and Traffic Engineering, Silesian University of Technology,
Krasińskiego 8, 40–019 Katowice, Poland,
E-mail: marcin.staniek@polsl.pl

Abstract. The paper presents the stereo vision method for the mapping of road pavement. The mapped road is a set of points in three-dimensional space. The proposed method of measurement and its implementation make it possible to generate a precise mapping of a road surface with a resolution of 1 mm in transverse, longitudinal and vertical dimensions. Such accurate mapping of the road is the effect of application of stereo images based on image processing technologies. The use of matching measure CoVar, at the stage of images matching, help eliminate corner detection and filter stereo images, maintaining the effectiveness of the algorithm mapping. The proper analysis of image-based data and application of mathematical transformations enable to determine many types of distresses such as potholes, patches, bleedings, cracks, ruts and roughness. The paper also aims at comparing the results of proposed solution and reference test-bench. The statistical analysis of the differences permits the judgment of error types.

Keywords: image processing, pavement distresses, road assessment, road inspection, road pavement conditions, stereo vision.

1. Introduction

The assessment of pavement conditions is the process of obtaining and processing information about road surface. The information is a set of operational parameters. Both the reliability and the accuracy are required to describe the conditions of road pavement.

Visual inspection of roads is the most popular method of monitoring the road pavement condition. Qualified inspectors who either walk or drive along the road and count distresses in the road surface carry it out. Despite its popularity, this type of road inspection features some drawbacks. In practice, this method is very slow, labour-consuming due to the visual measurement of damages and, consequently, it is costly. The description of road pavement condition is affected by the not fully objective approach of the inspectors who carry out the measurements. Such approach generates inconsistencies and inaccuracy of the representation. Furthermore, this type of road inspection represents a significant threat to the safety of inspectors because they work during high traffic intensity with vehicles often moving by at high speeds (Mustaffar *et al.* 2008).

In order to minimize the deficiencies of the visual method of collecting data on road pavement condition, it is necessary to implement automatic measurement systems. The application of modern technologies in road inspection appeared in a variety of studies. Yu *et al.* (2007) discussed a multi-sensor mobile system of laser scanning the road surface, which covers the width of 8 m. The main weakness of the scanning system was irregularity of measurements, which had to be interpolated, particularly in the locations with the lack of representation i.e. too smooth or wet surfaces.

Further, (Vilaça *et al.* 2010a, 2010b) the paper describes the solutions connected with the application of technologies of image processing and stereo vision for road inspection. Likewise, the studies presented a prototype of the device, which allows for acquisition of the data for the representation of the road surface using the system of two cameras and a laser pointer for evaluation of micro- and macrotexture of the road surface. The accuracy of measurements at the level of 0.5 mm was ensured by the proposed calibration procedure, which is extended, though time-consuming.

Grace *et al.* (2000) and He *et al.* (2010) proposed stereo vision methods for identification of the road potholes using a linear LED lighting or a projector that displays particular patterns. In the process of identification of damages, the deviations were measured between technical line obtained from an even surface and curved light line or deformed pattern. Measurement precision is maintained at the level of 5 mm.

Publication (Wang *et al.* 2004) presented stereo vision techniques for assessment of road pavement condition. It also demonstrated the opportunities of representation of transverse and longitudinal profile as well

doi:10.3846/bjrbe.2017.05

as identification of surface damages with the methods of area-based matching. The applied method of corner detection determined the measure of normalized cross-correlation of image areas. The authors of the study emphasize that the presented solution cannot be fully implemented in practice due to the equipment limitations.

Salari *et al.* (2012) introduced the application of suitable measures using the average sum of squares of intensity differences of corresponding pixels in matching stereo images. He also introduced the algorithm of background filtration for identification of surface damages and morphological transformations of images for the elimination of uneven illumination of the road. For identification of pavement damage in the areas with different colour or texture the SVM model was used.

Wang *et al.* (2011) and Wang (2011) proposed hybrid solutions of 2D and 3D systems for identification of the condition of road surface. The combination of linear 2D cameras, 3D cameras, and laser pointers allowed for connecting 2D representation (1 mm resolution) with the 3D representation of images. The weakness of this solution is that it necessitates dry road pavement condition during the measurements.

Reeves (2011) described the methodology and the device for determination of high-resolution road pavement maps, which provide input for the system of automated identification of road pavement condition i.e. identification of cracking, ruts and the road structure. The device consisted of linear cameras, set of LED lamps for illumination of the surface analysed, and module of lighting synchronization. To increase the accuracy of the map description, which represents road pavement condition, Reeves (2011) proposed both the system of surface condition identification and the system of model points determined with the use of the laser scanning. There was the suggestion to use the laser pointer for identification of the model points with the application of triangulation or LIDAR solution, which is a rotary laser-scanning device.

The following part of this article recommends using the stereo vision technique, which helps assess the road pavement conditions. The test-bench for identification of the road pavement condition has been developed. The analysis of the required parameters describing the road pavement condition take place. For the analysis it is necessary to take into consideration not only the comments of the inspectors who carry out measurements using different methods and measurement devices but also opportunities for using stereo vision techniques in the representation of road surface. With all the requirements, expectations, limitations and possibilities in mind, it has been possible to develop a mobile stereo vision test-bench used for road inspection.

2. Stereo vision techniques

Digital stereo vision is a technique that allows the recovery of 3D scenes from images (data set) obtained from at least two optoelectronic sensors. It is applied in industrial and medical diagnostics, vision quality control and manufacturing processes in industry, detection, and tracking of moving objects, in robotics, and virtual reality creations. The recent development in the field of Digital Signal Processor has made it possible to construct agile methods for both the automatic scene mapping and the object recognition on the 3D scene in the real-time processing (Di Stefano *et al.* 2004).

Specific stages of operating algorithm were chosen, i.e., implementation of transformations and calculations in images, which significantly simplify the presentation of the stereo vision processing. Fig. 1 presents the stages of stereo vision processing. In the first stage, two CCD cameras capture image sequences of the road surface. The capture parameters of the images are determined by a motion function of a measurement vehicle. The transfer of raw images to the pre-processing module takes place where two operations are executed (stage II): the lens distortion correction and the rectification of stereo images (Cyganek, Siebert 2009). To realize the second stage, it is necessary to perform the calibration process, which is carried out by the application of standard calibration pattern.

The method requires proper preparation of the pattern with defined dimensions and its description in the coordinates system. The road pavement is an XY plane of the coordinates system. Application of SUSAN edge detector (Qu *et al.* 2013) for the recognition procedure of reference points on the calibration pattern seems ideal. Locations of the reference points in the stereo images allow determining the function parameters of both correction and rectification for the processed images. The application of filtration procedure of stereo images by (Salari *et al.* 2012; Wang *et al.* 2011) is not appropriate for the described in this article solution. The use of filters changes the intensity values of pixels in the image (e.g. averaging for an area of the image), which consequently leads to the increase of differences in the intensity of the corresponding pixels of the stereo images. Such approach has a negative impact on matching procedure, which leads to incorrect mapping of the road surface.

Calculation of a disparity map of matching pixels is the third stage in stereo vision processing. The disparity map is a set of differences between each pair of pixels p_L and p_R for the reference image I_L and for the analysed image I_R. Generally, the two basic methods are used for determination of the disparity map: the direct method and the feature-based method. In the direct method, the function of image intensity is a measurable value determined for each location of the image. In the feature-based method, the detection of essential features of the image (e.g. corners or lines) follows. Then the objects recognized in stereo images are used in the process of determination of disparity maps.

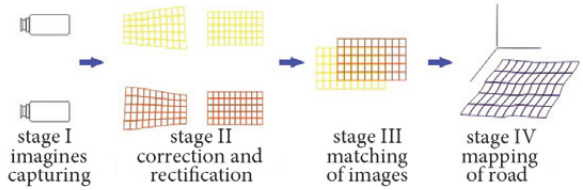

Fig. 1. The stages of stereo vision processing

Due to the necessity of representation of the road surface with the assumption of 1 mm^2 road equals 1 pixel of the image, it is necessary to adopt the direct method, which determines the dense disparity maps for the test-bench. The use of matching measure CoVar (Cyganek, Siebert 2009) determines the disparity map. The solutions of Wang *et al.* (2011) and Salari *et al.* (2012) were based on the normalized cross-correlation and the average sum of squares of differences of the corresponding pixels in stereo images. Additionally, the matching is made only of the objects extracted from the images identified with the use of Harris corner detector. Therefore, neither the identification procedure of the objects from images nor the proposed laser light projectors described in works of He *et al.* (2010), Wang *et al.* (2011) nor Reeves (2011) appear in this study.

In the proposed solution, the disparity map is determined for all points in stereo images. The measure for each pixel of the reference image I_L and the analysed image I_R is given by:

$$CoVar(m,\ n,\ d_m,\ d_n) = \frac{L(m,\ n,\ d_m,\ d_n)}{\sqrt{M_L(m,\ n)\cdot M_R(m,\ n,\ d_m,\ d_n)}}, \quad (1)$$

where *CoVar* – matching measure; m – horizontal coordinate of pixel; n – vertical coordinate of pixel; d_m – shift for horizontal coordinate of pixel; d_n – shift for vertical coordinate of pixel; L – item determined by Eq (2); M_L – item determined by Eq (3); M_R – item determined by Eq (4):

$$L(m,\ n,\ d_m,\ d_n) = \sum_{(i,j)\in U}\Big(\Big(I_L(m+i,\ n+j) - \overline{I_L(m,\ n)}\Big)\Big(I_R(m+d_m+i, n+d_n+j) - \overline{I_R(m,\ n,\ d_m,\ d_n)}\Big)\Big), \quad (2)$$

$$M_L(m,\ n) = \sum_{(i,j)\in U}\Big(I_L(m+i,n+j) - \overline{I_L(m,\ n)}\Big)^2, \quad (3)$$

$$M_R(m,\ n,\ d_m,\ d_n) = \sum_{(i,j)\in U}\Big(I_R(m+d_m+i,n+d_n+j) - \overline{I_R(m,\ n,\ d_m,\ d_n)}\Big)^2, \quad (4)$$

where I_L – reference image; I_R – analysed image; $\overline{I}_L$ –mean value of pixel for reference image area, Eq (6); $\overline{I}_R$ – mean value of pixel for analysed image area, Eq (7); U – determined image area:

$$U = \{(x,y): |x| \le 20 \cap x \in P,\ |y| \le 20 \cap y \in P\}, \quad (5)$$

where P – a set of integers.

$$\overline{I_L(m,\ n)} = \frac{1}{25}\sum_{(i,j)\in W} I_L(m-i,\ n-j), \quad (6)$$

$$\overline{I_R(m,\ n,\ d_m,\ d_n)} = \frac{1}{25}\sum_{(i,j)\in W} I_R(m-d_m-i, n-d_n-j), \quad (7)$$

where W – determined set of coordinates:

$$W = \{(x,y):\ x = -20,\ -10,\ 0,\ 10,\ 20,\ y = -20,\ -10,\ 0,\ 10,\ 20\}. \quad (8)$$

The search pixel with the coordinates $m+D_m$, $n+D_n$ of the analysed image area is determined by the maximum value of the matching measure *CoVar*:

$$\max_{d_m, d_n \in S} CoVar(m,\ n,\ d_m,\ d_n) \to D_m = d_m,\ D_n = d_n, \quad (9)$$

where: S – analysed stereo image area:

$$S = \{(x,y):\ |x| \le 30 \cap x \in P,\ |y| \le 10 \cap y \in P\}. \quad (10)$$

The proposed matching measure is more precise regardless of an extracted objects from the image than the ones cited above. Moreover, it is so accurate due to the identification of entire study area. Such approach is equivalent to the elimination of corner detection procedures and additionally to the removal of image filtering, adopted at the stage of pre-processing of images. The elimination allows for using efficient computational matching measure CoVar, however computationally more demanding, without increasing the complexity of the stereo vision system. Calculation of disparity maps, regardless of the adopted matching measures, is computationally complex and considered as disadvantageous in stereo vision systems.

The fourth stage in the stereo vision processing is the calculation of spatial representation of the road. The canonical camera system seems a better choice in the computational model, which means that the optical axes of the cameras are parallel and Z coordinate of the scheme is consistent with the focal length of one of the cameras. The road point and its mapping points (pixels) p_L and p_R, for the reference image I_L and for the analysed image I_R respectively, are marked in Fig. 2. Focal points c_L, c_R and the camera optical axes are marked in the figure as well. The information on the point projection of the stereo images is required to generate coordinates of road point H. With the disparity map, as well as the optical parameters of lens, and parameters of CCD matrices in use, it is possible to convert the stereo images into the spatial representation of road pavement. The coordinates of the road point H, which visible on the stereo images, are determined by:

$$H = \left\{(X,Y,Z):\ X = \frac{mo}{D_m + o},\ Y = \frac{no}{D_n + o},\ Z = \frac{ro}{v(D_m + o)}\right\}, \quad (11)$$

where H – coordinates of road point, mm; o – distance among the optical axes of the cameras, mm; r – focal length of the camera, mm; v – surface scaling coefficient.

For established algorithm of road mapping, the resolution of surface description equals 1 mm for each of three dimensions. Where necessary, the resolution is reduced or expanded by changing the parameters of mapping model (according to Eq (11)). However, the change affects the field size seen by cameras of the system. In basic image processing, without stereo vision dependence, the images present road pavement in graphic form (colour) and do not contain data relating to depth. In this case, the use of surface extraction filters on the image can lead to misidentification of plain dirt as the distress of road pavement. Stereo vision with the depth identification from images enables elimination of the extracted objects on the images (i.e. dirt surface) where no distresses of road pavement exist.

3. Implementation of the stereo vision measurement method

The developed test-bench consists of a set of optoelectronic devices, such as CCD cameras for the capture of stereo images of road pavement, and electronic devices for synchronization of the captured stereo images. In addition, electronic devices for identification of XYZ displacement of the test-bench, and devices for identification of the distance covered by the measurement vehicle appear in the proposed solution. An additional element of the test-bench is a GPS module for reading the current geographical location of the measurement vehicle and, combined with the system for road inspection, for determination of the distresses places in a road surface.

The frame of the test-bench is made of lightweight aluminium profiles with parts to help fix them to rear part of the bodywork of the measurement vehicle. The devices for identification of the distance covered are mounted on the wheel arch. The electronic devices for synchronization of stereo images and the device for recording the set of video data (stereo images recorder) are in the boot compartment of the vehicle. Fig. 3 shows the test-bench with one stereo cameras module for mapping the road pavement with the resolution of 1 mm in three dimensions. Red lines mark the field of view right side camera, the yellow lines – field of view of left side camera. Dark blue lines mark the boundaries of road surface mapping.

The movement of stereo cameras module in the left or right direction about the measurement vehicle is possible due to the use of frame on the test-bench, which record the wheel path in the system. In addition, it is feasible to increase the field size seen by cameras (entire traffic lane), but it also forces the decrease of resolution. Furthermore, the next stereo cameras module (the same as in Fig. 3) could be used, concurrently in the proposed system. In this case, the significant changes to measurement algorithm are not necessary.

Digital cameras DFK 31BU03.H manufactured by Imaging Source Europe GmbH equipped with sensitive 1/3″ Sony CCD ICX204AK sensor are used to build the stereo vision test-bench for road inspection They find their application in many solutions like industrial automation, quality assurance, security, surveillance and medical applications. The main feature of such industrial camera is low-cost and additional highly versatile imaging solution. According to the specific nature of these devices, CCD matrices used in these cameras record images with a resolution of 1024 pixels by 768 pixels of the image with the frame rate of 30 frames per second. The cameras have the external inputs for images triggering, and USB 2.0 interfaces for data transmission and work configuration of the device. The trigger inputs are crucial important because they allow for synchronized images capturing during road inspection while the measurement vehicle is moving.

The electronic device for synchronized stereo images capturing operates on the AVR microcontroller coupled with the device for identification of the distance covered. The rotation about the fixed angle of the vehicle wheel generates impulse for recording the next stereo images. The AVR microcontroller receives the impulses, codes them according to the specifications of the camera, and sends them to the trigger input for each camera at a particular point in time.

One defect of the test-bench is low parameters of the CCD matrices in the cameras, which record up to 30 frames per second. Exceeding the number of impulses over the threshold of the frame rate does not allow the whole research section of road pavement to be recorded

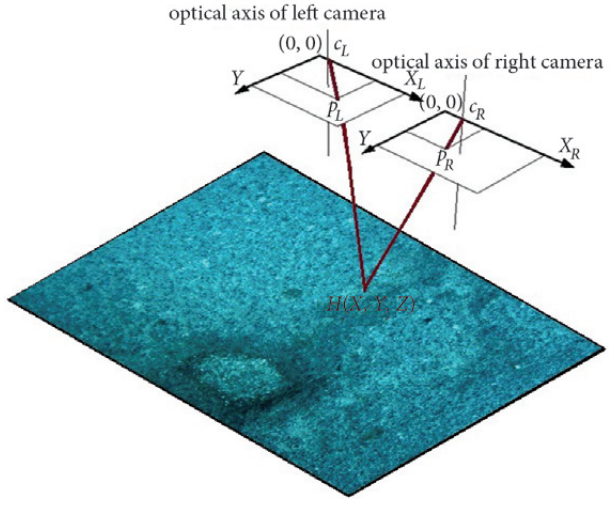

Fig. 2. Model of canonical system of stereo vision measurement

Fig. 3. Measurement vehicle with the stereo vision test-bench

but registers only the selected fragments. The continuity problem of the measurement does not exist for the speed lower than 80 km/h of the measurement vehicle (assuming the mapping of the road surface per image frame to be 1 mm^2 = 1 pixel). Once the speed of measurement vehicle is higher the mapping accuracy is not complete.

In case it is necessary to obtain the description of the whole 4 m long road cross section for the presented solution, the distance between cameras is stretched from 90 cm to 140 cm. After the change, such measurements are effective, but the resolution of the vertical plane is equal to 3 mm (for the solution presented in the paper the resolution is 1 mm). For the realization of measurements for the whole cross section (with resolution of 1 mm) the following two solutions are used: (1) replacement of the cameras for use with cameras with resolution of 1920 pixels by 1200 pixels or higher and (2) the use of two other modules mounted on the test-bench analogous to the one in Fig. 3.

The measurements of the road pavement condition are performed for selected sections of local roads during the period of low traffic intensity. The following figures present the example of a representation of the road surface using the stereo vision measurement method: Fig. 4a illustrates a direct image of road distress captured by cameras measuring system. Red lines in the illustration determine the field for mapping road pavement, Fig. 4b shows the depth map of road distress. The gradient of colour determines the deviation of an actual surface from the general plane, Fig. 4c presents the spatial model of mapped road pavement.

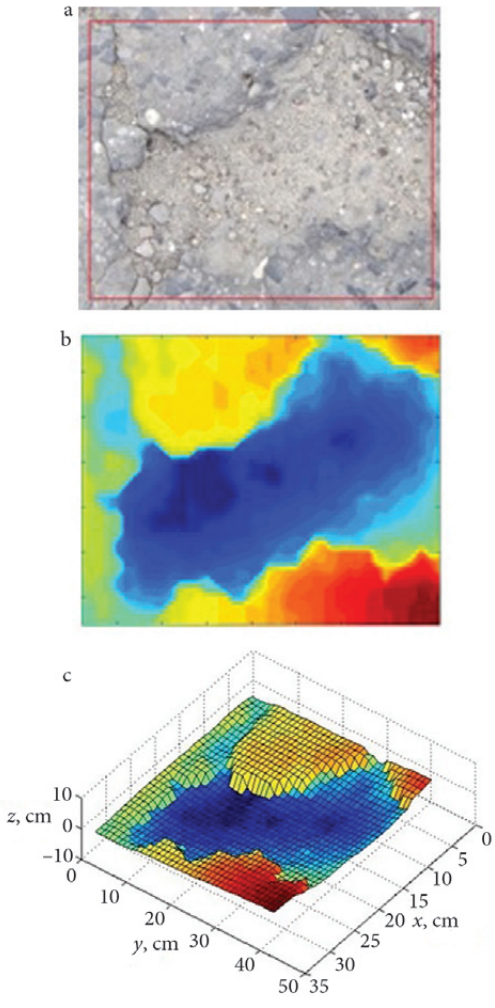

Fig. 4. Representation of the road surface: a – example image of road distress; b – depth map of road distress; c – spatial representation of mapped road distress

Mapping the road pavement with resolution 1 mm in 3D space is high precision measurements and enables the detailed description of road pavement conditions. The needs for data averaging or predicting are not necessary. That is the reason why the assessment method of road pavement conditions is practical and calls for direct measurements. Analysis of one set of surface data (3D map of the road) enables the identification of many types of distresses like potholes, patches, deformation, bleeding, cracks and ruts.

Identification of road distresses, and description of road pavement evaluation depend upon determining the deviations between the theoretical state of the road at a high level and the actual state of the road regarding linear or surface analysis. The deviations of the real profile of road from the theoretical profile in cases of transverse and longitudinal measurements represent rutting and roughness. The surface deviations represent distresses like potholes, patches, cracks, and bleedings. The method helps determine the deviations of measured actual road surface, and theoretical surface without any road distresses. The deviations observed in a narrow range on the plane, define the cracks. The application of the least square method supports the identification of technological cracks. The accepted methods of calculation for federal restrictions work to analyse the deviations, for example at a certain distance when the measurement vehicle is in movement.

4. Evaluation of stereo vision measurement method

The evaluation of the proposed measurement method is possible only when all the reference data from other measuring methods are gathered. They will constitute the baseline for the results obtained from stereo vision method. The application of 'yes' or 'no' checking procedure in case of the inventoried distresses for both measurement methods is insufficient. The result of stereo vision mapping is the 3D surface. In that stage comparison with the 3D reference surface is necessary. Popular vision systems of roads assessment using the image processing for the distresses identification are based on the single frame and do make it possible to determine the depth of the image. Typical laser profilograph for the evaluation of transverse profile enables to obtain the results with a resolution of 100 mm. Given the above and the need to carry out research under field conditions, it became necessary to develop a tool to describe the road pavement accurately. The tool will provide the appropriate reference data for evaluation of the achieved results of proposed stereo vision method.

The comparison of the obtained data set with the measurement data from the laser distance meter generates the evaluation of the stereo vision method of road surface

mapping. The reference test-bench design enables to carry out the measurements and mapping the road surface with high resolution in the *XY* plane on the road. Since experts conduct the road inspection during rush hours, short inspection and measurements time is advisable. Lightweight aluminium is used as the material for the reference test-bench, which allows for smooth movement on the *XY* surface of the measuring module in the plane 1100 mm by 850 mm. The position of the measuring module can varies with the resolution of 1 mm in both *X* and *Y*-axes because of the specification of road surface mapping. Laser distance meter Leica DISTRO D3a manufactured by Leica Geosystems AG is used to build the reference test-bench. The distance meter is a low-cost tool with a typical accuracy of ±1 mm confirmed by the producer certificate M by *DIN 55350-18-4.2.2*. Emitted wavelength equals 635 nm with a maximum radiant power smaller than 1mW. In addition, the reference test-bench is equipped with regulated legs to allow precise positioning in the horizontal plane about a mapped road surface. Fig. 5 presents the reference test-bench made to carry out the road surface mapping with laser techniques.

For precise mapping of road pavement, the measurements are performed when the vehicle is at a full stop i.e. there is no vibration of the test-bench. The vibration does not affect the description accuracy. In the evaluation process, it was assumed that the spatial description of the road with the use of a laser distance meter is accurate enough to stand comparison with the space description obtained from stereo vision method.

The comparison of the data from two measurement methods was performed to determine the differences between the measurement values. Eq (12) expresses the differences:

$$\Delta z(i,j) = z_l(i,j) - z_s(i,j), \tag{12}$$

where $\Delta z(i, j)$ – difference between the values of two measurements for the i^{th} measurement in the j^{th} measurement cross section, mm; $z_l(i, j)$ – result of the i^{th} measurement in the j^{th} measurement cross section for the laser distance meter, mm; $z_s(i, j)$ – result of the i-th measurement in the j^{th} measurement cross section for the stereo vision method, mm.

The performed distribution analysis of differences between measurements of the stereo vision methods and measurements from the laser distance meter have made it possible to check random errors obtained from the mapping of the road pavement. The selected statistical Shapiro-Wilk test has helped to verify the normal distribution of the differences between the two methods. Null hypothesis *H0* assumed that the differences between the measurements obtained with both methods have the normal distribution, whereas the alternative hypothesis *H1* assumes that the differences between the measurements do not have a normal distribution.

The significance level is assumed to equal $\alpha = 0.05$. Eq (13) gives the value of statistical test U_n for the Shapiro-Wilk test. The critical region in implementing the statistical test is the right side, defined as $[0, U_{crit}]$, where critical value is read from table (Taylor 1997).

$$U_n = \frac{\left[\sum_{i=1}^{n/2^*} a_{n-i+1}\left(X_{n-i+1} - X_i\right)\right]^2}{\sum_{i=1}^{n}\left(X_i - \overline{X}\right)^2}, \tag{13}$$

where U_n – statistical test of Shapiro-Wilk; X_i – number of differences Δz of i^{th} interval for ascending sorted elements; X_{n-i+1} – number of differences Δz of i^{th} interval for descending sorted elements; $\overline{X}$ – mean number of differences Δz for all intervals; a_{n-i+1} – Shapiro-Wilk coefficient for descending sorted elements, consistent with table (Taylor 1997); $n/2^*$ – integer part of $n/2$, n – number of intervals.

In addition, the correlation coefficient is determined for the measurements obtained from both measurement methods. The equation gives the coefficient for the j^{th} measurement cross section:

$$r(j) = \frac{\sum\left(\left(z_l(i,j) - \overline{z}_l(j)\right)\cdot\left(z_s(i,j) - \overline{z}_s(j)\right)\right)}{\sqrt{\sum\left(z_l(i,j) - \overline{z}_l(j)\right)^2 \cdot \left(z_s(i,j) - \overline{z}_s(j)\right)^2}}, \tag{14}$$

where $r(j)$ – correlation coefficient of the measurements in the j^{th} measurement cross section; $\overline{z}_l(j)$ – mean of the measurements in the j^{th} measurement cross section for laser distance meter, mm; $\overline{z}_s(j)$ – mean of the measurements in the j^{th} measurement cross section for stereo vision method, mm.

For the evaluation of the stereo vision in road inspection, it was necessary to assume the two types of measurements. The first type bases on measurements in a line according to the transverse profile of road and functions under the name collinear type of measurements. The second type contains the set of measurements in a horizontal plane under the name coplanar type of measurements.

Fig. 5. Reference test-bench with the laser distance meter

4.1. Collinear type of measurements

The collinear type of measurements test 160 measurement cross sections. The results of measurements come from the stereo vision method and the laser distance meter. Fig. 6 shows the graphic interpretation of differences $\Delta z(i, j)$ between the results of two measurement methods. The differences in collinear type of measurements are calculated for a sample of measurement cross-section. Horizontal axis describes set of locations of i-th measurements for the cross-section with resolution among successive measurement points of 5 mm. Vertical axis shows differences $\Delta z(i)$ for selected measurement cross section j.

Table 1 shows the verification of the statistical hypotheses for the selected measurement cross-sections, in the collinear type of measurements. 160 measurement cross sections are the subject of verification. However, the table presents only 27 most reliable and authoritative items. The $\Delta\overline{z}_i$ symbol indicates the mean value of the differences between the two measurement methods and the $\varphi\Delta z_i$ symbol indicates the standard deviation of the mean

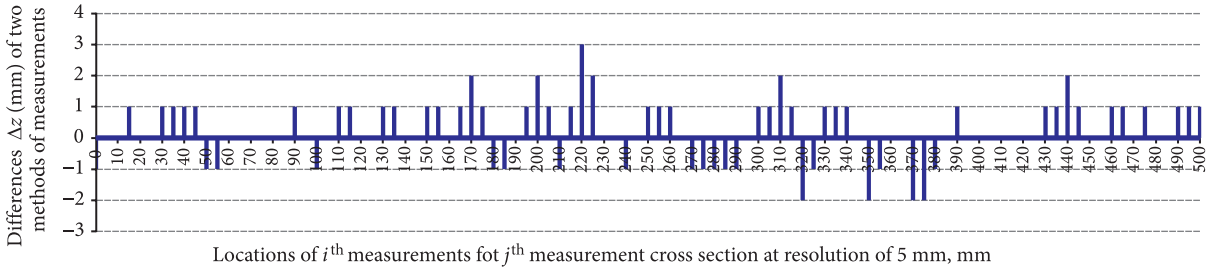

Fig. 6. Differences of two measurements methods in a sample of measurement cross section

Table 1. The results of analysis of the 27 selected measurement cross sections in the collinear type of measurements

j	$\Delta\overline{z}_i$	$\varphi\Delta z_i$	$d^-_{\max}$	$d^+_{\max}$	U_n	U_{crit}	n	r
1	−0.67	1.19	−3	3	0.896	0.803	7	0.941
2	−0.66	1.71	−5	3	0.895	0.829	9	0.968
3	−0.58	1.06	−4	2	0.884	0.803	7	0.916
4	−0.50	1.14	−3	2	0.888	0.788	6	0.912
5	−0.41	1.29	−3	3	0.905	0.803	7	0.901
6	−0.37	1.08	−3	2	0.918	0.788	6	0.901
7	−0.36	1.47	5	2	0.839	0.818	8	0.913
8	−0.33	1.29	−3	3	0.896	0.803	7	0.937
9	−0.29	1.19	−4	3	0.852	0.818	8	0.955
10	−0.07	0.99	−2	2	0.82	0.762	5	0.949
11	−0.01	1.33	−2	3	0.926	0.788	6	0.946
12	0.01	1.07	−3	2	0.872	0.788	6	0.991
13	0.15	1.55	−5	3	0.833	0.829	9	0.927
14	0.15	0.76	−2	2	0.876	0.762	5	0.984
15	0.16	1.07	−2	3	0.872	0.788	6	0.983
16	0.17	1.13	−3	3	0.908	0.803	7	0.970
17	0.18	1.02	−2	3	0.931	0.788	6	0.992
18	0.21	1.30	−4	4	0.835	0.829	9	0.908
19	0.21	0.97	−2	3	0.837	0.788	6	0.996
20	0.23	0.88	−2	2	0.837	0.762	5	0.911
21	0.28	1.49	−3	4	0.852	0.818	8	0.989
22	0.32	0.96	−3	2	0.879	0.788	6	0.977
23	0.33	1.31	−3	3	0.879	0.803	7	0.992
24	0.43	1.35	−3	4	0.899	0.818	8	0.934
25	0.45	1.22	−3	3	0.906	0.803	7	0.904
26	0.72	1.16	−2	3	0.876	0.788	6	0.950
27	1.00	1.11	−2	4	0.827	0.803	7	0.986

for the j^{th} measurement cross section. The maximum differences for the positive set and the negative set are indicated as d^{-}_{max} and d^{+}_{max}. The U_n symbol indicates the calculated value of Shapiro-Wilk test and U_{crit} symbol indicates critical value of test. The correlation coefficient is r.

The results for the verification of statistical hypotheses, in the collinear type of measurements, show that there is no evidence to reject the null hypothesis *H0* of normal distribution differences of measurements for the analysed research sections. Thus, no gross or systematic errors occur and only random ones are found. The symmetric distribution of the mean around zero confirms the randomness of the resulting errors. The resulting average values differences $\Delta\overline{z}_i$ for the j^{th} measurement cross section and the corresponding standard deviation $\varphi\Delta z_i$ confirm the precision of linear mapping in the stereo vision techniques of road inspection.

4.2. Coplanar type of measurements

The second type of measurements the coplanar type takes place in 110 different road points. The results of measurements for the horizontal plane come from the stereo vision method and the laser distance meter. The size of the plane is 800 mm by 500 mm with resolution 50 mm by 50 mm. Fig. 7 presents the example of the horizontal plane for measurements performed with laser distance meter where red lines mark the measurement surface.

Figure 8 shows the grids of measurements for the stereo vision method and the laser distance meter, respectively. In both figures presented below the horizontal plane (*ij*-plane) means the theoretical road surface without distresses (deviations) in the vertical direction (*z*-direction). The sample grids obtained with two measurement methods demonstrate the real road surface with a road distresses.

In the coplanar type of measurements, Fig. 9 shows the graphic interpretation of the differences Δz (i, j) between the two measurement methods of the sampled obtained grids. The values of differences Δz (i, j) are the result of subtraction – the values of the stereo vision measurement from the values of the laser distance meter.

The obtained measurements of the coplanar type have undergone thorough analysis as in the collinear type of measurements. The verification of statistical hypotheses has taken place to check the random errors of the measurements. Table 2 shows the analysis results of the selected road pavements for the coplanar type of measurements. The verification of 110 various places on roads has followed. However, the table presents only 17 most reliable and authoritative items. The symbols describe the same parameters as in the collinear type of measurements.

In the analysis, verification of statistical hypotheses for the coplanar type of measurements confirms normal distribution of the measurement differences. Thus, there are no gross errors or any systematic errors. There are only random errors with a symmetric distribution of the mean around zero (Taylor 1997). The obtained results confirm precision of the plane mapping in the proposed stereo vision method of road inspection.

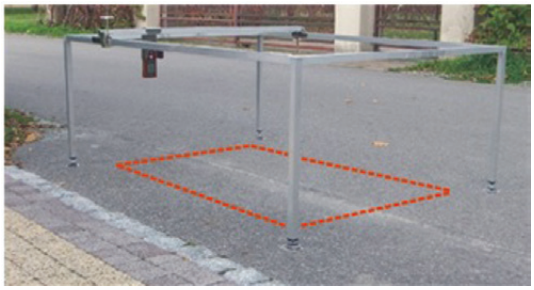

Fig. 7. Researched surface of road pavement

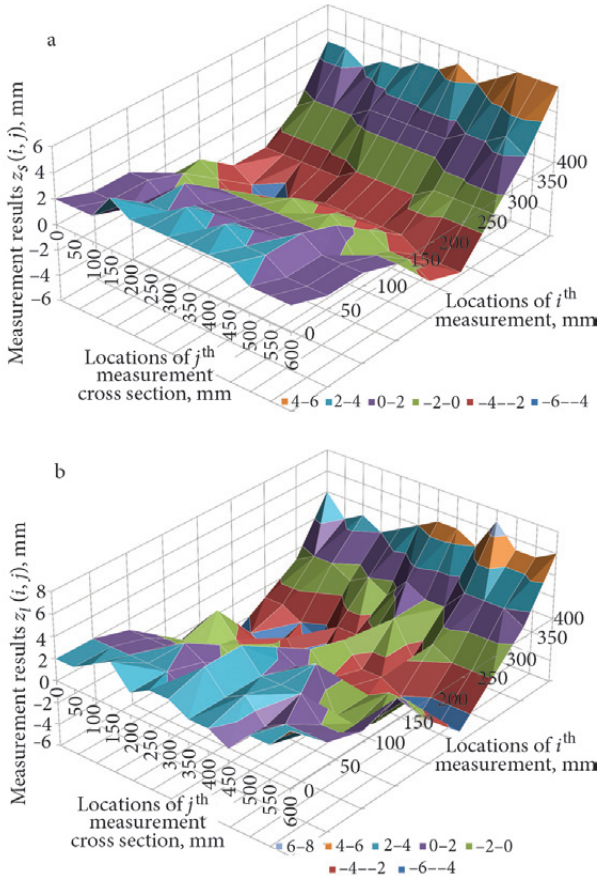

Fig. 8. Sample grid of measurements from: a – stereo vision method; b – laser distance meter

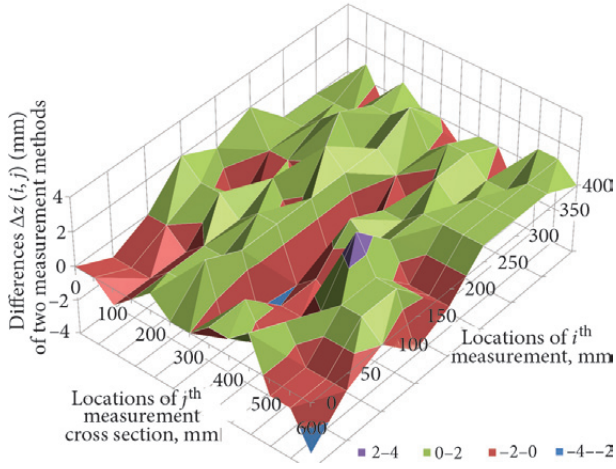

Fig. 9. Measurement differences between stereo vision method and laser distance meter

Table 2. The results of analysis of the seventeen selected measurement cross sections in the coplanar type of measurements

j	$\Delta\overline{z}_i$	$\varphi\Delta z_i$	$d^{-}_{\max}$	$d^{+}_{\max}$	U_n	U_{crit}	n	r
1	–0.195	1.634	–3	3	0.901	0.803	7	0.979
2	–0.181	1.923	–3	3	0.868	0.803	7	0.923
3	–0.176	1.497	–3	3	0.934	0.803	7	0.918
4	–0.13	1.523	–2	3	0.812	0.788	6	0.948
5	–0.104	1.082	–3	2	0.803	0.788	6	0.918
6	–0.079	1.201	–3	3	0.912	0.803	7	0.973
7	–0.045	1.467	–3	3	0.831	0.803	7	0.901
8	0.016	1.816	–3	3	0.876	0.803	7	0.901
9	0.021	1.469	–3	3	0.973	0.803	7	0.929
10	0.022	1.015	–3	2	0.843	0.788	6	0.934
11	0.038	1.198	–3	3	0.882	0.803	7	0.975
12	0.043	1.346	–3	3	0.834	0.803	7	0.946
13	0.057	1.206	–3	3	0.886	0.803	7	0.990
14	0.159	1.486	–2	3	0.799	0.788	6	0.927
15	0.184	1.529	–3	3	0.971	0.803	7	0.984
16	0.197	1.734	–3	2	0.869	0.788	6	0.967
17	0.203	1.397	–3	3	0.904	0.803	7	0.912

5. Conclusions

1. The proposed stereo vision method for road inspection successfully implements the matching measure CoVar. The application of the measure results in the elimination of both corner detection procedures and image filtering procedures. The elimination does not lead to malfunctioning of the road surface-mapping algorithm, which confirms the process of comparison measurements for two different types of measuring methods. The implementation of the matching measure CoVar does not lead to an increase in computational complexity of the whole measuring system due to the reserve of computational complexity, which is higher after the elimination of corner detection and image filtering procedures.

2. The constructed test-bench with cameras and developed algorithms for image processing for matching and mapping road pavement makes it possible to create a road map with a resolution of 1 mm in three dimensions. The obtained resolution provides high precision measurements and the possibility of the detailed description of road pavement conditions. In the proposed solution, the laser light projectors do not find their application in describing the condition of the road pavement at high resolution.

3. The measurements evaluation of stereo vision method undergoes verification on the 270 measurement cross sections, out of which 160 focus on the collinear type of measurements and 110 on coplanar type of measurements. Nearly 40 000 direct measurements are analysed. Irrespective of the measurement type, the means of differences set between the two measurement methods are around zero. Additionally, the calculated standard deviations for 270 measurement cross sections do not exceed 2 mm. Verification of statistical hypotheses confirm the randomness of errors and the fact that there are no gross or systematic errors. The calculated correlation coefficients confirm the dependence between measurements from stereo vision method and distance laser meter. For 270 researched samples the coefficients are not lower than 0.9.

4. The solution features high assessment speed, much lower time-consumption and lower costs per measurement procedure in comparison with the conventional methods. It is so because the measurements are made when the measurement vehicle is in motion, and qualified inspectors are not necessary for direct measurements on the road, which further increases the level of safety during the measurement time.

References

Cyganek, B.; Siebert, P. 2009. *An Introduction to 3D Computer Vision Techniques and Algorithms.* John Wiley & Sons, 504 p. https://doi.org/10.1002/9780470699720

Di Stefano, L.; Marchionni, M.; Mattoccia, S. 2004. A PC-Based Real-Time Stereo Vision System, *Machine Graphics & Vision* 13(3): 197–220.

Grace, A. E.; Pycock, D.; Tillotson, H. T.; Snaith, M. S. 2000. Active Shape from Stereo for Highway Inspection, *Machine Vision and Applications* 12(1): 7–15. https://doi.org/10.1007/s001380050119

He, Y.; Wang, J.; Qiu, H.; Zhang, W.; Xie, J. 2011. A Research of Pavement Potholes Detection Based on Three-Dimensional Projection Transformation, in *Proc. of the 4th International Congress on Image and Signal Processing (CISP 2011).* 15–17 October, 2011, Shanghai, China. 1805–1808. https://doi.org/10.1109/CISP.2011.6100646

Mustaffar, M.; Ling, T. C.; Puan, O. C. 2008. Automated Pavement Imaging Program for Pavement Cracks Classification and Quantification – a Photogrammetric Approach, in *Proc. of the 21st International Society for Photogrammetry and Remote Sensing (ISPRS 2008)*: 37(B4). Ed. by Chen, J.; Jiang, J.; Nayak, Sh. 3–11 July, 2008, Beijing, China. 367–372.

Qu, Z.; Gao, Y.; Wang, P.; Shen, Z. 2013. Fast SUSAN Edge Detector by Adapting Step-Size, *Optic – International Journal for Light and Electron Optics* 124(8): 747–750. https://doi.org/10.1016/j.ijleo.2012.01.026

Reeves, B. 2011. *High Speed Photometric Stereo Pavement Scanner.* Patent No. WO2011069191A1, EP2510307 A1, US2013 0076871, published in 16 June, 2011.

Salari, E.; Chou, E.; Lynch, J. J. 2012. *Pavement Distress Evaluation Using 3D Depth Information from Stereo Vision*. Final Report. MIOH UTC TS43.

Taylor, J. R. 1997. *An Introduction to Error Analysis: the Study of Uncertainties in Physical Measurements.* 2nd edition. University Science Books, 349 p.

Vilaça, J. L.; Fonseca, J. C.; Pinho, A. C. M. 2010a. Non-Contact 3D Acquisition System Based on Stereo Vision and Laser Triangulation, *Machine Vision and Applications:* 21(3): 341–350. https://doi.org/10.1007/s00138-008-0166-7

Vilaça, J. L.; Fonseca, J. C.; Pinho, A. C. M.; Freitas, E. 2010b. 3D Surface Profile Equipment for the Characterization of the Pavement Texture – TexScan, *Mechatronics:* 20(6): 674–685. https://doi.org/10.1016/j.mechatronics.2010.07.008

Wang, K. C. P. 2011. Elements of Automated Survey of Pavements and a 3D Methodology, *Journal of Modern Transportation* 19(1): 51–57. https://doi.org/10.1007/BF03325740

Wang, K. C. P.; Gong, W.; Tracy, T.; Nguyen, V. 2011. *Automated Survey of Pavement Distress Based on 2D and 3D Laser Images*, *MBTC DOT 3023 – Grant*.

Wang, K. C. P.; Gong, W.; Elliott, R. P. 2004. A Feasibility Study on Data Automation for Comprehensive Pavement Condition Survey, in *Proc. of the 6th International Conference on Managing Pavements*. 19–24 October, 2004, Brisbane, Australia.

Yu, S.; Sukumar, S. R; Koschan, A. F.; Page, D. L.; Abidi, M. A. 2007. 3D Reconstruction of Road Surfaces Using an Integrated Multi-Sensory Approach, *Optics and Lasers in Engineering* 45(7): 808–818. https://doi.org/10.1016/j.optlaseng.2006.12.007

Received 15 May 2014; accepted 14 December 2015